Biochemistry & Analytical Biochemistry
ISSN: 2161-1009

Das et al., Biochem Anal Biochem 2017, 6:1
DOI: 10.4172/2161-1009.1000310

Research Article Open Access

Graphene: A Building Foundation for Efficient Plasmonic SERS Device

Gobind Das*, Manola Morett, Bruno Torre, Marco Allione, Andrea Giugni and Enzo Di Fabrizio

Physical Sciences and Engineering (PSE), King Abdullah University of Science and Technology (KAUST), Kingdom of Saudi Arabia

Abstract

In this paper graphene over SiO_2/Si substrate was used as a substrate to fabricate SERS device. A thin film was deposited over graphene and annealed at 250°C. The substrate was examined after chemisorption of two molecules; rhodamine 6G which is a fluorescent dye, and 3-mercaptobenzoic acid, a thiol molecule. SERS enhancement factor for the proposed device is estimated to be 2.1×10^6 with respect to the flat silver substrate deposited over Si. The experimental results were compared in two ways; a) by using electromagnetic field calculation and b) quantum mechanical calculation derived from density function theory. The experimental findings were consistent with the theoretical observations.

Introduction

Graphene, a planar atomic layer of carbon atoms organized hexagonally, is the center of research efforts because of its exceptional electrical, mechanical, and optical properties [1-5]. The optical and mechanical properties keep the graphene in the front line of research associated to thin-film transistors, photonics, micro-/nanomechanical system [6-8]. In the field of photonics, graphene gained a remarkable importance due to its applications ranging from analytical sensor to light-emitting devices and lasers to photodetectors [9]. Herein, we demonstrate the graphene based Surface enhanced Raman scattering (SERS) device as an efficient analytical sensor.

SERS is an analytical technique, which provides the fingerprint of molecular bonds despite the intrinsic weak Raman signal [10]. It is being widely employed in order to have high surface sensitivity and giant signal enhancement [11]. There are two main factors associated to the increase in Raman signal: localization of electric field (in the range of 10^6 to 10^8) due to the presence of plasmonic hot-spots and the chemical effect (usually in the range of 10^2) which involves a charge transfer between metal and the chemical compound in its close proximity. When an electromagnetic radiation is exposed over it, results a huge enhancement in Raman signal. SERS effect, in combination with proper designed SERS substrate and Raman spectroscopy, augments the sensitivity of the analytical measurements [12].

SERS devices were fabricated by means of different techniques: e.g. electron beam lithography (EBL), optical lithography, electrochemical methods, anodic porous alumina template assisted, or a combination of different techniques (EBL and electroless, focused ion beam lithography and optical lithography), etc. [13-17]. For manufacturing the above-mentioned devices, one needs different sophisticated instruments and many fabrication steps. All these processes and multistep production techniques result in an increase in the price tag of the overall devices. The optical properties of the nanostructures (size and shape) determine the efficiency of the device and the final experimental results, i.e., changing the shape and size of the nanostructure leads to a variation in the optical response [18,19]. It is always a bottleneck demand to have a uniform, reproducible, highly sensitive and cost effective SERS substrate available [20,21]. Few efforts were made in the past utilizing graphene surface for SERS applications [22-24]. In the current work, we mainly focus on the nanotailoring or nanoassembly of devices with a uniform distribution of metal nanoparticles exploiting a graphene based SERS design. The clear, sharp and well-studied Raman fingerprints of graphene (as a function of number of layers, laser excitation frequency, etc.) facilitates the molecular analysis as the Raman spectrum contains only one intense Raman band at around 1600 cm^{-1} in the region of importance from 400-2000 cm^{-1} [25,26].

In this work, a fast and simple technique is employed to fabricate SERS devices. A graphene layer is used as a building base for SERS devices. Single-layer graphene (SLG) coated with silver is used here to employ a simplified fabrication process for plasmonic application. The devices were thereafter annealed at sintering temperature (T_s) of 250°C, leads to an increase in average Ag nanoparticle size [27-31]. As prepared (AsPrep) and annealed (As250) samples were analyzed by means of atomic force microscopy (AFM) technique. The SERS activity of devices was investigated using rhodamine 6G (Rd6G) and 3-mercapto benzoic acid (3-MBA) molecules. The SERS substrate (graphene and silver nanoparticles) behaves as an active biosensor, providing an enhanced Raman intensity and, at the same time, a fluorescence quenching substrate [32,33].

Experimental Procedure

Device fabrication

SLG on SiO_2/Si substrate was purchased from Fisher Scientific – USA. Silver metal of 8 nm thickness was deposited by means of bench-top sputtering technique (Quorum Technologies, model: Q150T). The deposition rate was fixed to 0.5A/s. The sample is thus termed as AsPrep_GAg. AsPrep_GAg sample was then annealed at the sintering temperature of 250°C for 1h dwell time under controlled N_2 atmosphere, thus labeled As250_GAg. Two kinds of samples (AsPrep_GAg and As250_GAg) were then analyzed by AFM techniques. The schematic representation of sample preparation for spectroscopic analysis is shown in Figure S1 (Supplementary information: S1).

The devices were, thereafter, immersed in the molecular solution (Rd6G in water and 3-MBA in ethanol from Sigma) and let chemisorb for 30 minutes at room temperature. The device was then gently rinsed with the respective solvent to wash out excess molecules that are not directly attached to the metal surface. Afterwards, the sample was

***Corresponding author:** Gobind Das, Physical Sciences and Engineering (PSE), King Abdullah University of Science and Technology (KAUST), Thuwal 23955-6900, Kingdom of Saudi Arabia, Tel: +966128020185; E-mail: gobind.das@kaust.edu.sa

Received: December 19, 2016; **Accepted:** March 02, 2017; **Published** March 06, 2017

Citation: Das G, Morett M, Torre B, Allione M, Giugni A, et al. (2017) Graphene: A Building Foundation for Efficient Plasmonic SERS Device. Biochem Anal Biochem 6: 310. doi: 10.4172/2161-1009.1000310

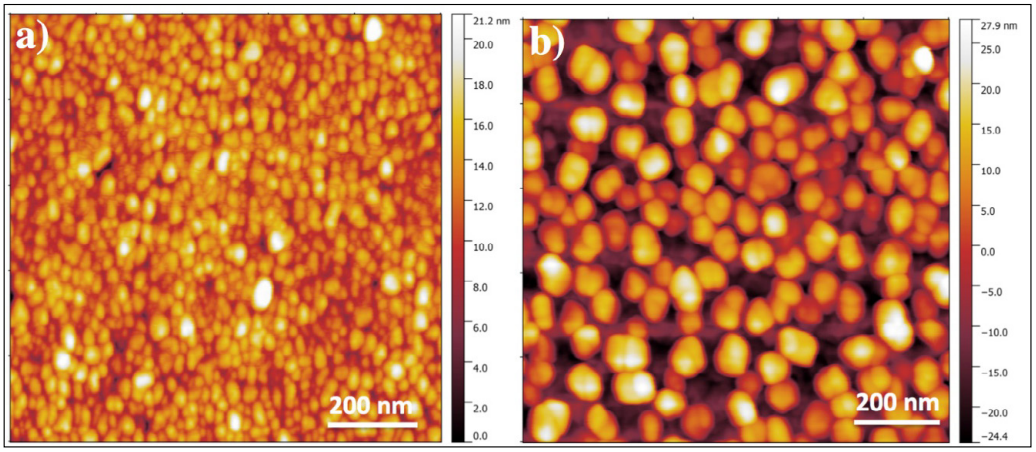

Figure 1: AFM image of SERS samples: a) AsPrep_GAg (sample after metal deposition on graphene film) and b) As250_GAg (AsPrep_GAg sample after annealing at 250°C for one hour dwell time).

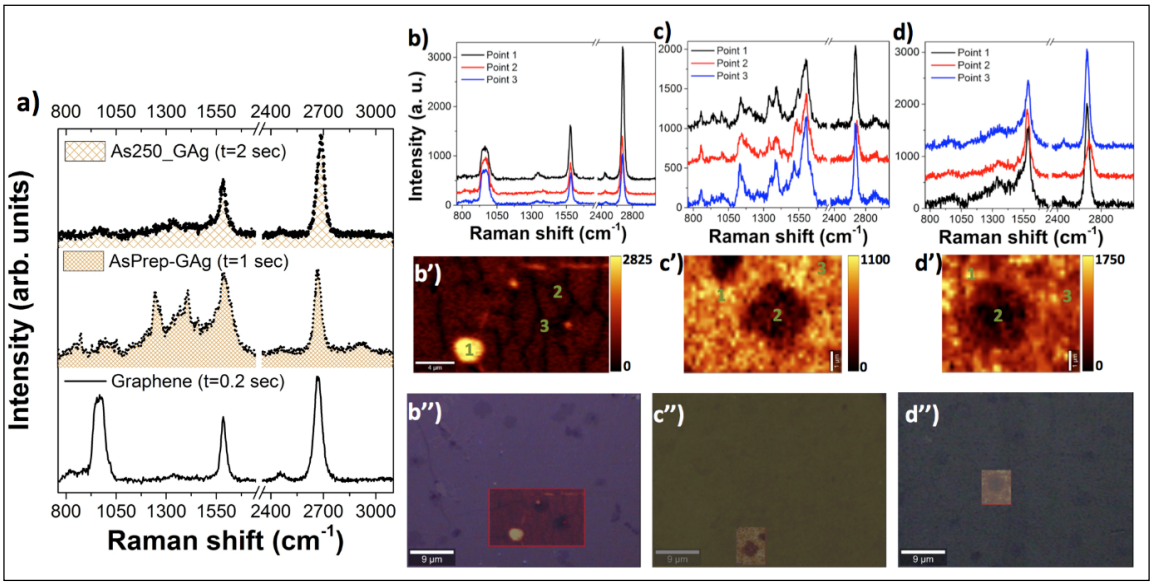

Figure 2: Raman spectra of Graphene, Graphene coated with silver metal, and Graphene coated with silver annealed at 250°C. The filling pattern under the curve symbolizes the particle's size and density. In addition, three sets, b), c) and d), are related to the virgin Graphene, AsPrep_GAg and As250_GAg, respectively. From bottom to top panel: the optical image of the sample overlapped with the mapping analysis, the mapping analysis for the vibration band centered at 2674 cm^{-1}, and the Raman spectra at three different locations (marked in mapping analysis image). The measurements were performed with the exposure time 0.003 sec, 0.05 sec and 0.15 sec, respectively. Laser power was kept constant for all the measurements. The spectra were baseline corrected.

dried under nitrogen flow. Now the sample is ready to investigate the molecules of interest.

Characterization technique

AFM measurements on AsPrep_GAg and As250_GAg samples were carried out by means of Asylum Research Instrument (model: MFP_3D-Bio AFM). The samples were measured before and after annealing in tapping mode by means of Mikromasch probes (HQ-XSC11, tip c,) of 15570 kHz nominal resonance frequency and nominal spring constant 2 N/m) for a topography scanning areas of 1 × 1 um^2. The following statistical quantities were calculated: for AsPrep_GAg, rms roughness of 2.06 nm and average particle radius of 10.1 ± 5.7 nm; and for As250_Gag, rms rougness of 9.12 nm and average particle radius of 18.6 ± 9.1 nm. AFM images of these two devices are shown in Figure 1.

Micro-probe Raman measurements were performed by WiTec Alpha 300RA. The system was equipped with 600 grooves/mm, objective 100 X (NA: 0.9), EMCCD detector to achieve the well dispersed intense Raman signal. The whole system was placed on active vibration platform to avoid any interference from surrounding movements. The molecules were excited by 532.0 nm laser wavelength in backscattering configuration. The samples were investigated before and after measurements to assure no conformational changes by laser exposure. Spectral analysis was carried out using WiTec Project 4, commercial software.

Density function theory (DFT) calculation was performed for a free molecule and for the molecule attached to silver for SERS configuration. In case of Ag attached molecule, the metal particle was attached to the thiol group releasing H atom [34]. The calculations were carried out using the commercially available ADF2016 package. The molecule was

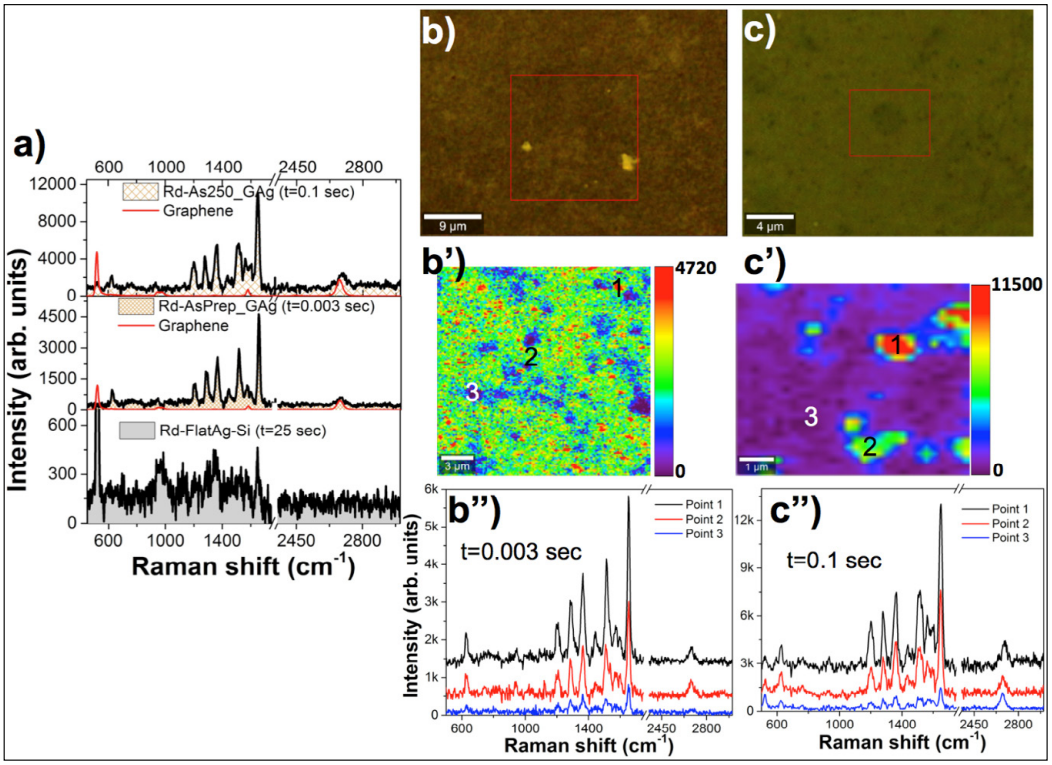

Figure 3: a) SERS spectra of Rd6G deposited over silver coated Si substrate (t=25 sec, a reference spectrum), AsPrep_GAg (t=0.003 sec) and As250_GAg (t=0.1 sec) (from bottom to top). Red curves of SLG are inserted for comparison. Optical image of mapping area, SERS mapping analysis of band@1655 cm^{-1} of Rd-AsPrep_GAg sample (b, b', b'') and of Rd-As250_GAg sample (c, c', c''). The integration time for Rd-AsPrep_GAg and Rd-As250_GAg is 0.003 and 0.1 sec, respectively. Laser power was fixed for all the measurements.

firstly optimized in its geometry considering and thereafter Raman bands were estimated using generalized gradient approximations (GGA) of Perdew-Burke-Emzerhof (PBE) exchange functional and TZP basis set.

Results and Discussion

The Raman spectra of graphene sample, before and after Ag metal deposition, are shown in Figure 2. Micro-Raman spectrum of SLG on SiO_2/Si substrate shows clear contribution from two characteristic G and 2D bands, centred at 1585.2 and 2674 cm^{-1}, respectively [35]. No D band is found in Raman spectrum of virgin graphene sample. A broad band is observed in the range of 900-1050 cm^{-1} which can be attributed to the second order of Si substrate. After metal sputtering, the appearance of few spectral features in the spectral range below 1500 cm^{-1} (in the range of 1300-1400 cm^{-1}) and at the same time an increase in the band width of G-band can be attributed to the introduction of defects sites due to the sputtering. Liu et al. observed similar behavior, when the researchers deposited Aluminum (Al) by means of sputtering technique [36]. It is plausible that silver atoms, in our case, during the sputtering process retain high kinetic energy, transferred to the graphene sheet. This leads to the creation of carbon vacancies or defect site. Raman band due to disorder can be observed in Figure 2b in the spectral region of 1300-1480 cm^{-1}. However, the G and 2D bands of graphene start emerging (and disappearance of D band) as observed in Figure 2c after annealing AsPrep-GAg sample at 250°C. It could be possible because the sample may be recovering the defects after annealing at high temperature. In the past it is reported that the defect sites could be recovered when annealed at around 900°C [37] but in our case the annealing temperature is lower. It could be due to the presence of Ag nanoparticles on graphene, which are playing a vital role. A sharp 'G' band and minimum disorder 'D' band contribution return into effect. Micro-Raman mapping measurements were performed on all the samples, shown in Figure 2. The set of Figures 2b-2d is related to the virgin Graphene, AsPrep_GAg, and As250_GAg samples, respectively. From lower to top panel, the optical image of the sample, the mapping analysis of sample centered around 2674 cm^{-1} and the Raman spectrum of three associated points mentioned in middle panel were shown in the Figure. The mapping analysis shows a similar behavior as shown in Figure 2a.

Two different molecules (Rd6G, a fluorescent molecule, and 3-MBA, a thiol molecule) were extensively examined for SERS activity after deposition over silver coated substrates. The step size during the mapping measurement was maintained around 300 nm.

Rhodamine 6G, a fluorescent molecule, is being often used to investigate the functionality of SERS device because of two major reasons: to inspect the fluorescence quenching that will diminish the fluorescence background of the Raman spectrum; and to illustrate the chemical fingerprint of the molecule with enhanced Raman intensity of the vibrational bands. SERS measurements for Rd6G (50 nM), deposited over silver coated SLG samples and over silver coated Si substrate, were performed in the spectral range of 450 – 3000 cm^{-1}, shown in Figure 3a. The spectra were baseline corrected using the Project 4 (WiTec software). The fingerprint vibrational bands of Rd6G were clearly visible at around 1650, 1575, 1513, 1364, 1285, and 1208 cm^{-1} [38,39]. One sharp band, observed at around 521.5 cm^{-1} for FlatAg_Si sample, is due to the Si substrate underneath of Ag surface. The comparative spectra show an increase in Rd6G SERS intensity though the measurement

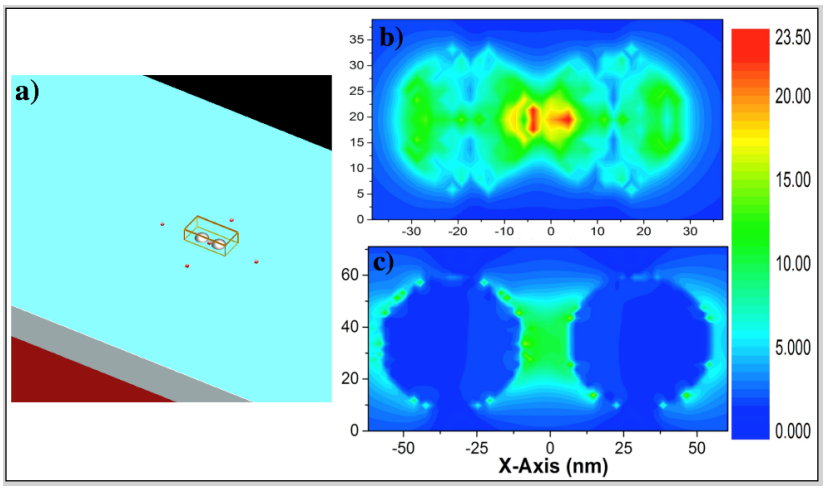

Figure 4: a) Design of device dimer. Red color represents Si wafer, gray is related to SiO_2 and light blue color is graphene. Dimers are shown in the center of design; Electric field distribution for the dimer with b) radius 12 nm and gap 8 nm, c) radius 25 nm and gap 15 nm.

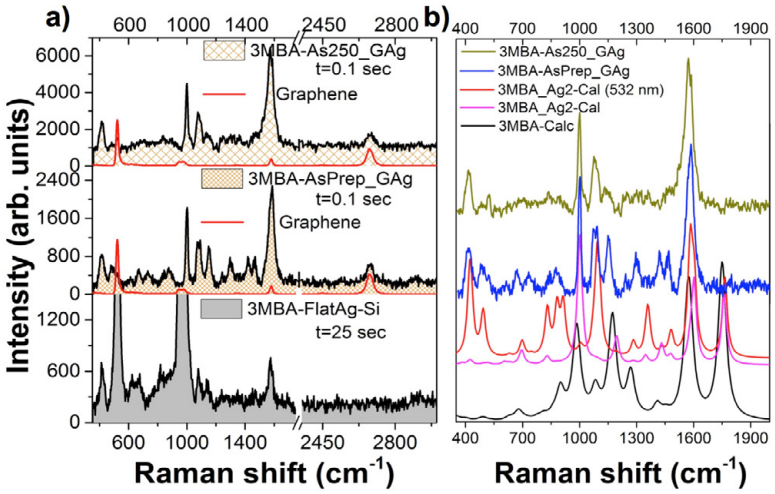

Figure 5: a) SERS spectra of 3MBA chemisorbed over 3MBA-As250_GAg, 3MBA-AsPrep_GAg and 3MBA-FlatAg-Si substrate, respectively (from top to bottom). Red curves of SLG are inserted for direct comparison; b) theoretical and experimental Raman spectra of 3MBA free and chemisorbed over Ag. Two calculated Raman spectra were reported one excited with 532 nm and with its default frequency.

parameters (integration time, laser power and Raman active area) were reduced remarkably. The mapping measurements were also performed to inspect the distribution of plasmonic hot-spots through out the mapping area (18 × 18 um^2). The optical image, mapping analysis for Raman band centred at 1655 cm^{-1}, and SERS spectra of Rd6G at three points (points are indicated by numbers), deposited over AsPrep_GAg and As250_GAg samples, were shown in Figures 3b, 3b', 3b" and 3c, 3c', 3c", respectively. In case of AsPrep_GAg device, the plasmonic hot-spot distribution can be revealed throughout the mapping area whereas in case of As250_GAg, the hot-spots are very much confined at limited space. This exhibits the presence of small gap (of around 5 nm) between two small nanoparticles over the substrate. The annealing of sample at sintering temperature leads to an increment in nanoparticle size and the reduction in the number of hot-spots. SERS enhancement factor for Ag coated over graphene surface samples, AsPrep_GAg and As250_GAg, is found to be 2.1 × 10^6 and 7.2 ×10^5, respectively, with respect to the flat Ag surface over Si substrate (see supplementary information: S2).

To confirm the above statement of high electric field confinement, finite difference time domain (FDTD) simulation was carried out using Lumerical commercial package. The design of fabricated device, shown in Figure 4a, was made in such a way that it resembles the experimental one. The comparative study was made for device; dimer consisting of 12 nm radius Ag nanoparticles with gap of 8 nm, and the Ag nanoparticles dimer with radius and gap of 25 and 15 nm, respectively. The mesh resolution of the device simulation was kept 2 × 2 × 2 nm^3. A linearly polarized light with wavelength of 532 nm was employed for both simulations. The maximum electric field in case of 25 nm radius was found much lower with respect to the device with radius of 12 nm, as shown in Figures 4b and 4c). The theoretical findings were found in complete accordance with the experimental findings.

Furthermore, 3-MBA molecule was examined over different devices; flat Ag, AsPrep_GAg and As250_GAg. Various intense Raman bands, finger-print of 3-MBA, were observed in the spectral range of 350 – 3000 cm^{-1} as shown in Figure 5a [40,41]. The vibrational band at

520 cm^{-1} is related to the Si substrate underneath Ag coating. Intense peak centred at 420, 1001, 1084 and 1152 cm^{-1} can be attributed to the C-S stretching, in-plane symmetry ring breathing, the combination of C-S stretching and in-plane ring deformation, and in-plane C-H deformation, respectively. The vibration band around 1580 cm^{-1} corresponds to the combination of G-band of graphene and the C-C stretching of benzene ring, whereas the peak at around 2670 cm^{-1} is related to the 2D-band of graphene. Since 2D band (zone-boundary phonon) in graphene is always very intense with respect to G band (first order graphene band) [26,42], the presence of intense peak at around 1580 cm^{-1} in case of sputtered samples is due to the MBA rather than graphene placed underneath the molecule.

The occurrence of plasmonic hot-spots was revealed throughout the mapping area, shown in 2D mapping analysis for 2 bands centred at 1585 and 1001 cm^{-1} (see supplementary information: S3 Figure S32). The band centred at around 1000 cm^{-1} is only due to 3-MBA while the band around 1585 cm^{-1} has dominant contribution from 3-MBA with respect to the graphene. However, it is observed that the intensity of major bands of 3MBA in case of As250_GAg is much pronounced than what is observed for AsPrep_GAg. This could be due to the possible shift in resonance peak resulting from convolution of molecular resonance and localized surface plasmon resonance.

Density functional theory (DFT) calculation

Amsterdam Density Functional (ADF) package was used to carry out all the calculations for interested molecules. DFT calculation was made for 3MBA as a free molecule and when attached to the silver surface. Optimized geometry of both with and without chemisorption to silver is shown in Figure S3 (see supplementary information: section S4). Generalized gradient approximations (GGA) of Perdew-Burke-Emzerhof (PBE) exchange functional in addition to TZP basis set was used for all the calculations. In addition, highest occupied molecular orbital (HOMO) and lowest unoccupied molecular orbital (LUMO) were also evaluated to explain the enhancement mechanism of SERS spectra (see supplementary information: S4). The energy gap between HOMO to LUMO for molecule with and without Ag was found to be 1.28 eV and 3.17 eV, respectively. Raman spectra of 3MBA with and without silver attached were also calculated, shown in Figure 5b. The molecular dynamics calculations, with (red colored spectrum) and without (pink colored spectrum) mentioning an excitation laser wavelength, were made for 3MBA attached to silver. We have employed the laser wavelength fixed to 532 nm in case of red colored spectrum. Experimental SERS results for the samples, 3MBA-As250_GAg and 3MBA-AsPrep_GAg, were compared with calculated Raman spectra for free molecule and for silver attached molecules. Calculated Raman peaks can be observed coherent with the SERS spectra of 3MBA molecule attached with silver. In the experimental observation, C=O and S-H vibrations were suppressed. Various vibration Raman bands can be observed at around 1585, doublet 1430-1470, 1296, 1150, 1076, 1000, doublet 880-840, 670, and doublet at around 492-421 cm^{-1} which can be attributed to aromatic C-C vibration, C-H bending, combination of C-C bending and C-H bending, symmetric CCO^{-}, C-C (aromatic) bending, combination of symmetric C-S and C-C, aromatic breathing, combination of asymmetric C-S and C-C, bending aromatic, combination of O-H and C-S bending, respectively.

The above experimental and calculated findings confirm the graphene coated with silver metal functions as a plasmonic SERS device. However, it has been found that AsPrep device works in a superior manner when chemisorbed with Rd6G whereas the annealed device for 3-MBA. This could be due to the variation of the combined effect of plasmonic and molecular resonance.

Conclusion

Graphene template is employed to fabricate fast and effective SERS device after depositing 6 nm of silver metal by means of sputtering technique. Two devices were prepared; AsPrep and annealed at 250°C. The devices were then chemisorbed with Rd6G (a fluorescent molecule) and 3-MBA (thiol molecule) to investigate the functioning as a SERS substrate. SERS enhancement factor was estimated to be 2.1 $\times$ 10^6. DFT calculation was also made to compare the SERS result of 3-MBA molecule. The results show the consistency in experimental and calculated one. Further investigation is needed to optimize efficient SERS samples by varying the annealing temperature.

Acknowledgement

GD acknowledges KAUST research computing system for their valuable support for ADF calculations.

References

1. Wang D, Choi D, Li J, Yang Z, Nie Z, et al. (2009) Self-assembled TiO_2–graphene hybrid nanostructures for enhanced Li-ion insertion. ACS Nano 3: 907-914.
2. Frank IW, Tanenbaum DM, Van der Zande AM, McEuen PL (2007) Mechanical properties of suspended graphene sheets. J Vac Sci Technol B 25: 2558-2561.
3. Griep MH, Sandoz-Rosado E, Tumlin TM, Wetzel E (2016) Enhanced graphene mechanical properties through ultrasmooth copper growth substrates. Nano Letters 16: 1657-1662.
4. Yong-Jin K, Yuna K, Konstantin N, Byung HH (2015) Engineering electrical properties of graphene: Chemical approaches. 2D Materials 2: 042001.
5. Bonaccorso F, Sun Z, Hasan T, Ferrari AC (2010) Graphene photonics and optoelectronics. Nat Phot 4: 611-622.
6. Bolotin KI, Sikes KJ, Jiang Z, Klima M, Fudenberg G, et al. (2008) Ultrahigh electron mobility in suspended graphene. Solid St Commun 146: 351-355.
7. Echtermeyer TJ, Lemme MC, Bolten J, Baus M, Ramsteiner M, et al. (2007) Graphene field-effect devices. Eur Phys J Spec Top 148: 19-26.
8. Schwierz F (2010) Graphene transistors. Nat Nanotechnol 5: 487-496.
9. Gan X, Mak KF, Gao Y, You Y, Hatami F, et al. (2012) Strong enhancement of light–matter interaction in graphene coupled to a photonic crystal nanocavity. Nano Letters 12: 5626-5631.
10. Kneipp K, Yang W, Kneipp H, Perelman LT, Itzkan I, et al. (1997) Single molecule detection using surface-enhanced raman scattering (SERS). Phys Rev Lett 78: 1667.
11. Das G, Battista E, Manzo G, Causa F, Netti PA, et al. (2015) Large-scale plasmonic nanocones array for spectroscopy detection. ACS Appl Mater Interfaces 7: 23597-23604.
12. Das G, Chirumamilla M, Toma A, Gopalakrishnan A, Zaccaria RP, et al. (2013) Plasmon based biosensor for distinguishing different peptides mutation states. Sci Rep 3: 1792.
13. Chirumamilla M, Das G, Toma A, Gopalakrishnan A, Zaccaria RP, et al. (2012) Optimization and characterization of Au cuboid nanostructures as a SERS device for sensing applications. Microelectron Eng 97: 189-192.
14. Perney NMB, Baumberg JJ, Zoorob ME, Charlton MDB, Mahnkopf S, et al. (2006) Tuning localized plasmons in nanostructured substrates for surface-enhanced Raman scattering. Opt Exp 14: 847-857.
15. Das G, Patra N, Gopalakrishanan A, Proietti ZR, Toma A, et al. (2012) Surface enhanced Raman scattering substrate based on gold-coated anodic porous alumina template. Microelectron Eng 97: 383-386.
16. Coluccio ML, Gentile F, Das G, Nicastri A, Perri AM, et al. (2015) Detection of single amino acid mutation in human breast cancer by disordered plasmonic self-similar chain. Sci Adv 1: e1500487.
17. Das G, Alrasheed S, Coluccio ML, Gentile F, Nicastri A, et al. (2016) Few molecule SERS detection using nanolens based plasmonic nanostructure: application to point mutation detection. RSC Adv 6: 107916-107923.
18. Haynes CL, McFarland AD, Duyne RPV (2005) Surface-enhanced raman spectroscopy. Anal Chem 77: 338A-346A.

19. Kyeong-Seok LM, El-Sayed A (2006) Gold and silver nanoparticles in sensing and imaging: Sensitivity of plasmon response to size, shape, and metal composition. J Phys Chem B 110: 19220-19225.

20. Das G, Patra N, Gopalakrishnan A, Zaccaria RP, Toma A, et al. (2012) Fabrication of large-area ordered and reproducible nanostructures for SERS biosensor application. Analyst 137: 1785-1792.

21. Biggs KB, Camden JP, Anker JN, Duyne RPV (2009) Surface-enhanced raman spectroscopy of benzenethiol adsorbed from the gas phase onto silver film over nanosphere surfaces: Determination of the sticking probability and detection limit time. J Phys Chem A 113: 4581-4586.

22. Xu W, Ling X, Xiao J, Dresselhaus MS, Kong J, et al. (2012) Surface enhanced Raman spectroscopy on a flat graphene surface. Proc Nat Acad Sci 109: 9281-9286.

23. Kang L, Chu J, Zhao H, Xu P, Sun M (2015) Recent progress in the applications of graphene in surface-enhanced Raman scattering and plasmon-induced catalytic reactions. J Mat Chem C 3: 9024-9037.

24. Yu X, Tao J, Shen Y, Liang G, Liu T, et al. (2014) A metal-dielectric-graphene sandwich for surface enhanced Raman spectroscopy. Nanoscale 6: 9925-9929.

25. Klar P, Lidorikis E, Eckmann A, Verzhbitskiy IA, Ferrari AC, et al. (2013) Raman scattering efficiency of graphene. Phys Rev B 87: 205435.

26. Ferrari AC, Basko DM (2013) Raman spectroscopy as a versatile tool for studying the properties of graphene. Nat Nanotechn 8: 235-246.

27. Pinkhasova P, Chen H, Verhoeven MWGM, Sukhishvili S, Du H (2013) Thermally annealed Ag nanoparticles on anodized aluminium oxide for SERS sensing. RSC Adv 3: 17954-17961.

28. Meškinis Š, Čiegis A, Vasiliauskas A, Šlapikas K, Gudaitis R, et al. (2016) Annealing effects on structure and optical properties of diamond-like carbon films containing silver. Nanoscale Res Lett 11: 146.

29. Suzuki Y, Ojima Y, Fukui Y, Fazyia H, Sagisaka K (2007) Post-annealing temperature dependence of infrared absorption enhancement of polymer on evaporated silver films. Thin Solid Films 515: 3073-3078.

30. Ma L, Huang Y, Hou M, Li J, Zhang Z (2016) Pinhole effect on the melting behavior of Ag@Al_2O_3 SERS substrates. Nanoscale Res Lett 11: 170.

31. Hajakbari F, Ensandoust M, (2016) Study of thermal annealing effect on the properties of silver thin films prepared by DC magnetron sputtering. Acta Physica Polonica A 129: 680-682.

32. Anger P, Bharadwaj P, Novotny L (2006) Enhancement and quenching of single-molecule fluorescence. Phys Rev Lett 96: 113002.

33. Dulkeith E, Morteani AC, Niedereichholz T, Klar TA, Feldmann J, et al. (2002) Fluorescence quenching of dye molecules near gold nanoparticles: Radiative and nonradiative effects. Phys Rev Lett 89: 203002.

34. Shao Y, Li C, Feng Y, Lin W (2013) Surface-enhanced Raman scattering and density functional theory study of 1,4-benzenedithiol and its silver complexes. Spectrochim Acta Part A: Mol Biomol Spectrosc 116: 214-219.

35. Srivastava A, Galande C, Ci L, Song L, Rai C, et al. (2010) Novel liquid precursor-based facile synthesis of large-area continuous, single, and few-layer graphene films. Chem Mater 22: 3457-3461.

36. Liu W, Wei J, Sun X, Yu H (2013) A study on graphene-metal contact. Crystals 3: 257-274.

37. Chen J, Shi T, Cai T, Xu T, Sun L, et al. (2013) Self healing of defected graphene. Appl Phys Lett 102: 103107.

38. Coluccio ML, Das G, Mecarini F, Gentile F, Pujia A, et al. (2009) Silver-based surface enhanced Raman scattering (SERS) substrate fabrication using nanolithography and site selective electroless deposition. Microelectron Eng 86: 1085-1088.

39. Sadegh N, Khadem H, Tavassoli SH (2016) High Raman-to-fluorescence ratio of Rhodamine 6G excited with 532 nm laser wavelength using a closely packed, self-assembled monolayer of silver nanoparticles. Appl Opt 55: 6125-6129.

40. Velleman L, Bruneel JL, Guillaume F, Losic D, Shapter JG (2011) Raman spectroscopy probing of self-assembled monolayers inside the pores of gold nanotube membranes. Phys Chem Chem Phys 13: 19587-19593.

41. Kim JH, Kang H, Kim S, Jun BH, Kang T, et al. (2011) Encoding peptide sequences with surface-enhanced Raman spectroscopic nanoparticles. Chem Commun 47: 2306-2308.

42. Malard LM, Pimenta MA, Dresselhaus G, Dresselhaus MS (2009) Raman spectroscopy in graphene. Phys Rep 473: 51-87.